Two-Photon Coincident-Frequency Entanglement via Extended Phase Matching

Onur Kuzucu, Marco Fiorentino, Marius A. Albota, Franco N. C. Wong, and Franz X. Kärtner

Research Laboratory of Electronics, Massachusetts Institute of Technology, Cambridge, Massachusetts 02139, USA
(Received 26 October 2004; published 1 March 2005)

We demonstrate a new class of frequency-entangled states generated via spontaneous parametric down-conversion under extended phase-matching conditions. Biphoton entanglement with coincident signal and idler frequencies is observed over a broad bandwidth in periodically poled KTiOPO$_4$. We demonstrate high visibility in Hong-Ou-Mandel interferometric measurements under pulsed pumping without spectral filtering, which indicates excellent frequency indistinguishability between the down-converted photons. The coincident-frequency entanglement source is useful for quantum information processing and quantum measurement applications.

Improvement in measurement accuracies beyond the classical limits is one of the most attractive applications of quantum entanglement. For example, one can perform two-photon interferometric measurements with sensitivity better than the diffraction limit by exploiting the momentum entanglement of photon pairs generated from spontaneous parametric down-conversion (SPDC) [1]. Recently, Giovannetti *et al.* [2] suggested that timing and positioning measurements can be enhanced by $\sqrt{N}$ over the standard quantum limit $\Delta t = 1/\sqrt{N}\Delta\omega$ if one uses the N-photon coincident-frequency-entangled state, with mean frequency $\overline{\omega}$, $|\psi\rangle = \int d\omega \phi(\omega)|\overline{\omega} + \omega\rangle_1 \ldots |\overline{\omega} + \omega\rangle_N$, where $\phi(\omega)$ is the spectral amplitude, Δt is the timing accuracy, and $\Delta\omega$ is the coherence bandwidth of each photon. For the simplest nontrivial case of $N = 2$ the coincident-frequency-entangled state $|\psi\rangle_{\text{CF}} = \int d\omega \phi(\omega)|\overline{\omega} + \omega\rangle_1|\overline{\omega} + \omega\rangle_2$ consists of a pair of entangled photons with identical but uncertain frequencies; the two photons are positively correlated in frequency, and hence anticorrelated in time. In contrast, conventional SPDC, the most common method for generating entangled photon pairs, typically yields pairs of time-entangled photons that are correlated in time but anticorrelated in frequencies as described by the state $|\psi\rangle_{\text{SPDC}} = \int d\omega \phi(\omega)|\overline{\omega} + \omega\rangle_1|\overline{\omega} - \omega\rangle_2$. As a result, SPDC under conventional phase-matching condition is not suitable for generating coincident-frequency entanglement.

The ability to generate a coincident-frequency-entangled state also provides a solution to the problem of frequency distinguishability in pulsed SPDC. This problem is particularly relevant when pulsed pumped SPDC is used to increase temporal resolution in timing or other measurement applications. Because of the large pump bandwidth and frequency anticorrelation in the down-converted light, pulsed SPDC typically generates photon pairs with signal and idler frequency spectra that are not identical [3]. This spectral distinguishability under pulsed pumping causes Hong-Ou-Mandel (HOM) interferometric measurements [4] to have poor visibility [5]. Coincident-frequency entanglement, on the other hand, yields photon pairs with the

same spectral properties, thereby restoring the HOM visibility. This type of entanglement can be used in a broad variety of applications ranging from linear optics quantum computing [6] to timing measurements [2].

We note that pulsed polarization entanglement with high visibility has been previously demonstrated in a dual-port SPDC configuration that separates the signal and idler fields at the output [7]. Because the signal and idler fields are not mixed, their polarization entanglement is not sensitive to the difference in their spectra, a concept that is used in bidirectionally pumped SPDC with interferometric combination [8]. However, such techniques would still show low HOM visibility under pulsed pumping because the spectra of the interfering photons are different.

Several groups recently suggested the possibility of generating a biphoton output that approximates the two-photon coincident-frequency-entangled state $|\psi\rangle_{\text{cf}}$ by engineering the SPDC phase-matching function [9–12]. In this Letter we report on the experimental generation of two-photon coincident-frequency entanglement by use of extended phase matching (EPM) in type-II phase-matched periodically poled KTiOPO$_4$ (PPKTP), as proposed by Giovannetti *et al.* [11,12]. We obtain high HOM visibility under pulsed pumping with a pulse width shorter than the biphoton coherence time. The EPM technique eliminates the degradation in HOM visibility associated with a long crystal under pulsed pumping. This technique should lead to better entanglement sources for quantum applications such as cryptography, teleportation, and quantum computing, as well as timing measurements.

For entanglement generation via SPDC, one is mostly interested in the frequency degenerate case in which the signal and idler frequencies are equal to half of the pump frequency. Therefore, we assume degenerate collinear down-conversion at pump frequency ω_p with the phase mismatch $\Delta k \equiv k_p(\omega_p) - k_s(\omega_p/2) - k_i(\omega_p/2) = 0$, where $k_{p,s,i}$ are the moduli of the wavevectors in the crystal for the pump (p), signal (s), and idler (i). When the pump frequency is tuned, Δk is no longer zero for a frequency degenerate output. This can be rectified if we operate at a

point where the phase mismatch's first frequency derivative $\Delta k' = \partial(\Delta k)/\partial\omega$ is also zero, which yields $k'_p(\omega_p) = (k'_s(\omega_p/2) + k'_i(\omega_p/2))/2$. The conditions $\Delta k = 0$ and $\Delta k' = 0$ are called extended phase matching [11,12]. The consequence of EPM is that the phase-matched signal and idler frequencies remain equal as ω_p is tuned or if a pulsed pump is used. This remains true if the pump tuning range or the pump bandwidth Ω_p is smaller than the extended phase-matching bandwidth Ω_{EPM}, which is determined by the second frequency derivative of Δk [12]. Because k' is the inverse of the group velocity EPM is also known as zero group velocity mismatch in ultrafast nonlinear optics.

Our coincident-frequency entanglement generation method is conceptually simple. In addition to operating under EPM conditions, we use a long crystal of length L to narrow the phase-matching bandwidth whose full width at half maximum is

$$\Omega_c = \frac{2\pi}{|k'_s - k'_i|L}. \tag{1}$$

Type-II phase matching is used so that $k'_s \neq k'_i$ and a small Ω_c can be obtained for coincident-frequency output $\omega_s \approx \omega_i$. The phase-matching bandwidth Ω_c is related to the biphoton coherence time $\tau_c = 2\pi/\Omega_c = |k'_s - k'_i|L$. The coincident-frequency-entangled state $|\psi\rangle_{cf}$ is generated if [12]

$$\Omega_c \ll \Omega_p \ll \Omega_{\mathrm{EPM}}, \tag{2}$$

which ensures that the HOM visibility is unaffected by pulsed pumping.

We have chosen a 10 mm long PPKTP crystal for coincident-frequency generation. Periodic poling in PPKTP allows one to use the grating period as a free parameter for phase matching at any set of operating wavelengths within the crystal's transparency window. Thus, we can always choose a grating period to satisfy the effective conventional phase-matching condition $\Delta k = 0$. For noncritical type-II phase matching with collinear propagation along the crystal's x axis, $\Delta k'$ is entirely determined by the dispersion of the crystal. Recently we have experimentally determined that for a pump wavelength $\lambda_p \approx 792$ nm the EPM conditions for degenerate collinear type-II phase matching are satisfied with a grating period of ~ 46.15 μm [13]. Using this PPKTP crystal we demonstrated efficient ultrabroadband second harmonic generation over an EPM bandwidth of 67 nm centered at the fundamental wavelength of ~ 1584 nm. This bandwidth is nearly 2 orders of magnitude larger than typical second harmonic generation bandwidths.

Figure 1 shows the experimental setup for the generation of coincident-frequency entanglement and the HOM interferometric analysis. The pump was a Ti:sapphire laser (Spectra-Physics, Tsunami) that could be operated in either continuous-wave (cw) or pulsed mode without altering its output spatial mode characteristics. In pulsed operation, the mode-locked laser output had a 3 dB bandwidth of
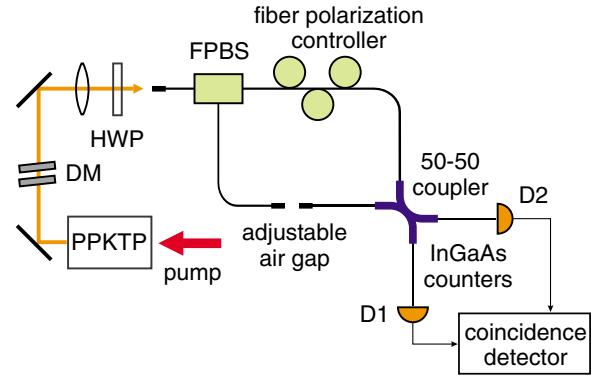

FIG. 1 (color online). Experimental setup showing the entanglement source and the fiber HOM interferometer used to test the coincidence-frequency-entangled state. DM: dichroic mirror, HWP: half-wave plate, FPBS: fiber polarization beam splitter.

~ 6 nm and an average power of 350 mW at an 80 MHz pulse repetition rate. The PPKTP crystal was antireflection coated at 792 and 1584 nm and the pump light was focused into it with a diameter of ~ 200 μm. The output was collimated and two dichroic mirrors (reflecting the 792 nm pump and transmitting the 1584 nm signal and idler) were used to eliminate the pump and no narrowband spectral filtering was used to restrict the output bandwidth. The resultant output was then focused into a single-mode polarization-maintaining (PM) optical fiber for subsequent HOM interferometric measurements.

The fiber-coupled light was sent to a fiber polarizing beam splitter (FPBS) that separated the orthogonally polarized signal and idler photons into their respective fiber channels. A half-wave plate (HWP) at the entrance to the PM fiber was used to set up the signal and idler in their appropriate fiber polarization modes. In the signal arm of the HOM interferometer was a fiber polarization rotator that was used to match the idler polarization in the second arm. The two arm lengths between the FPBS and the 50-50 fiber coupler were carefully matched by including an adjustable air gap in the idler arm. The air gap was nominally 50 mm long and efficient coupling (> 70%) between the two fibers was achieved by attaching a collimator to each fiber.

The two outputs of the 50-50 coupler were sent to two fiber-coupled custom-made InGaAs single-photon counters. The design and performance of similar devices have been described in more detail in our previous work [14,15]. The InGaAs detectors were operated in Geiger mode by simultaneously sending a 20 ns gating pulse (3.9 V above the breakdown voltage) to each detector at a repetition rate of 50 kHz, yielding a detector duty cycle of 10^{-3}. The counter D1 (D2) had a detection quantum efficiency of 16% (24%) at ~ 1580 nm. Under the above operating conditions we measured dark count rates of 40/s and 20/s for D1 and D2, respectively, which correspond to dark count probabilities of 8×10^{-4} (D1) and 4×10^{-4} (D2) per gate. The photocount outputs were amplified and

sent into a high-speed AND-gate logic circuit for coincidence detection within a 1.8 ns coincidence window. For cw pumping with 350 mW pump power, we have observed average singles count probabilities of 2.3×10^{-3} (D1) and 2.5×10^{-3} (D2) per 20 ns gate, corresponding to count rates of 125/s and 115/s, respectively (not corrected for dark counts). The probability of detecting a pair per gate is 2×10^{-5} corresponding to a count rate of 1 coincidence/s. The low coincidence count rate is due to the interferometer losses ($\sim 65\%$ transmissivity, measured independently), low detector quantum efficiencies, and an estimated 30% coupling efficiency into the PM fiber. From the detection efficiencies and our measurement duty cycle we estimate a single spatial fiber-optic mode pair production rate of $\sim 4 \times 10^6/s$ at 350 mW of pump power.

For the HOM measurements, the coincidence counts and the two singles counts were measured as a function of the air gap distance. Accidental coincidence counts were separately measured by using the same technique described in Refs. [14,15]. Typical accidental coincidence probabilities within the 1.8 ns coincidence window were 5×10^{-7} per gate corresponding to 5 counts in a 200 s measurement time. Figs. 2 and 3 show the data corrected for the accidental counts.

Figure 2 shows the HOM measurements under cw pumping at the pump wavelength of 792 nm, and we obtained similar results at a different pump wavelength of 787 nm. The biphoton coherence time is related to the base-to-base width of the HOM dip l_c by $\tau_c = l_c/2c$. Fitting the experimental data with the HOM triangular dip expected for type-II phase matching yields a visibility of $95 \pm 5\%$ and a biphoton coherence time of 1.42 ± 0.26 ps, which is equivalent to a biphoton coherence bandwidth of 2.5 ± 0.4 nm. The measured coherence bandwidth is in excellent agreement with the 2.5 nm bandwidth calculated from PPKTP's Sellmeier equations

[13]. The HOM visibility is defined by $V = 1 - C_{min}/C_{max}$, where C_{min} is the coincident count at zero signal-idler time delay and C_{max} is the coincident count at a long time delay (in the flat part of the HOM measurement). The fiber-to-fiber coupling efficiency of the air gap varied by $\sim 10\%$ over the scan, and we normalize the coincidence data to the maximum singles count rate in Figs. 2 and 3; this normalization affects the visibility by $\sim 1\%$. The cw measurements represent the first demonstration of tunable SPDC without any degradation of the biphoton entanglement, a result due to the large extended phase-matching bandwidth of 67 nm. The tuning range of 10 nm centered at the wavelength of 1584 nm is 4 times larger than the coherence bandwidth. We measured that the FPBS had an extinction ratio of $\sim 99\%$ for both ports. A 2% reduction in the visibility is caused by the 1% leakage of the signal field into the idler channel and vice versa. This 2% loss could be eliminated by using a clean-up polarizer in each of the two output ports of the FPBS.

For the pulsed HOM measurement, the setup was identical to that used in the cw measurements, except the pump laser was set in the pulsed mode centered at 790 nm with a 3 dB bandwidth of 6 nm. Figure 3 shows the pulsed HOM measurement results with a visibility of $85 \pm 7\%$ and a biphoton coherence time $\tau_c = 1.3 \pm 0.3$ ps. This is the first observation of high HOM visibility, without spectral filtering, in pulsed SPDC in which the pump bandwidth Ω_p is much larger than the biphoton coherence bandwidth Ω_c. The visibility in pulsed HOM is sensitive to deviations from the exact EPM operating conditions such as the crystal angle (affecting the effective grating period) and the pump wavelength. The slightly lower visibility in pulsed HOM results compared with the cw measurements may be caused by such deviations. Another plausible explanation for the lower visibility in pulsed HOM interferometry is the presence of higher order terms in the phase-
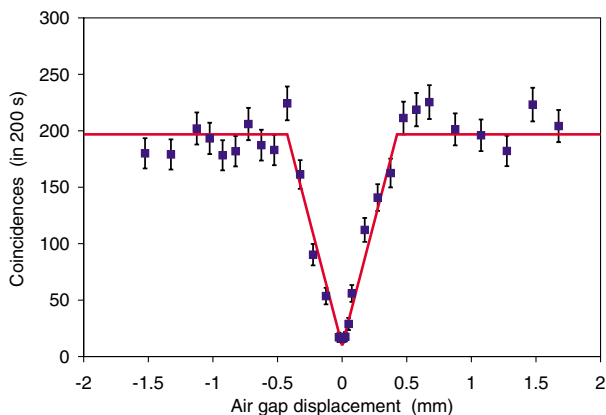

FIG. 2 (color online). HOM interferometric measurements under cw pumping at 792 nm. The experimental data are fitted with a triangular-dip HOM function (solid line). Base-to-base width of the HOM dip is $l_c = 0.85 \pm 0.16$ mm corresponding to a biphoton coherence time $\tau_c = 1.42 \pm 0.26$ ps. HOM dip visibility is $95 \pm 5\%$.
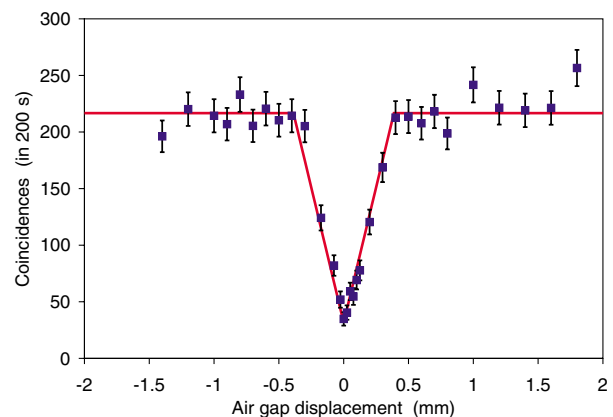

FIG. 3 (color online). HOM interferometric measurements for a pulsed pump centered at 790 nm with a 3 dB bandwidth of 6 nm. The experimental data are fitted with a triangular-dip HOM function (solid line). Base-to-base width of the HOM dip is $l_c = 0.8 \pm 0.2$ mm corresponding to a biphoton coherence time $\tau_c = 1.3 \pm 0.3$ ps. HOM dip visibility is $85 \pm 7\%$.

matching function that have not been considered in theoretical analyses [11,12].

We also measured the autocorrelation of the signal and idler light. The PPKTP output light was sent through a polarizer to pass only the horizontally polarized signal or the vertically polarized idler photons, then rotated by 45° with a second HWP before being coupled into the fiber interferometer. The fiber interferometer, as depicted in the setup of Fig. 1, became effectively a Mach-Zehnder interferometer because the FPBS now served as a 50-50 beam splitter for the input signal or idler light. The autocorrelation measurement shows a signal coherence time of 380 fs, and an idler coherence time of 350 fs, which are much shorter than the biphoton coherence time of 1.3 ± 0.3 ps.

The high visibility obtained in our pulsed HOM measurements is the consequence of operating under EPM which allows for the generation of coincident-frequency entanglement. The signal and idler outputs are frequency entangled if, given the generic biphoton state $|\psi\rangle_{BI} = \int\int d\omega_s d\omega_i A(\omega_s, \omega_i)|\omega_s\rangle|\omega_i\rangle$, the spectral amplitude $A(\omega_s, \omega_i)$ cannot be factorized as $f_s(\omega_s)f_i(\omega_i)$ [16]. If the two photons are not entangled, then $S_s(\omega_s) = |f_s(\omega_s)|^2$ and $S_i(\omega_i) = |f_i(\omega_i)|^2$ are the fluorescence spectra, which are directly related to their coherence times. If the two interfering photons at the 50-50 coupler of the HOM setup were not entangled, such as those from two single-photon sources, the HOM coherence time would be given by the overlap integral of the two pulses, as shown in Refs. [4,17,18]. In our case, the pulsed biphoton coherence time of 1.3 ps is much longer than the single-photon coherence times, which are less than 400 fs. Such a long biphoton coherence time would not be possible if the two photons were not entangled. The large difference between the measured biphoton coherence time and the single-photon coherence times suggests a significant amount of frequency entanglement. However, we believe that the output state was not maximally entangled. Such a non-maximally entangled output state is consistent with our observations: a small reduction in HOM visibility and a slightly shorter HOM coherence time compared with the cw results. Further measurements and theoretical analyses are needed to clarify the effects of various pump and crystal parameters on the amount of entanglement and HOM visibilities.

In summary, we have demonstrated a new technique of generating entangled photons with coincident frequencies in parametric down-conversion under extended phase-matching conditions. HOM interferometric measurements show high visibilities for cw or pulsed pumping, valid for a broad tuning range or pump pulse bandwidth that is less than the large extended phase-matching bandwidth. Pumping the crystal bidirectionally (as shown in [8]) under EPM would allow us to generate photons that are both coincident-frequency and polarization entangled. Pulsed entanglement provided by this quantum state suits the needs of linear optics quantum computing experiments, which require high timing resolution and high quality interference [6]. Also, timing and positioning measurements can be improved by $\sqrt{2}$ over the standard quantum limit if coincident-frequency-entangled photons are used in time-of-arrival measurements [2].

[1] A. N. Boto *et al.*, Phys. Rev. Lett. **85**, 2733 (2000); M. D'Angelo, M. V. Chekhova, and Y. Shih, *ibid.* **87**, 013602 (2001); R. S. Bennink, S. J. Bentley, R. W. Boyd, and J. C. Howell, *ibid.* **92**, 033601 (2004).

[2] V. Giovannetti, S. Lloyd, and L. Maccone, Nature (London) **412**, 417 (2001); Phys. Rev. A **65**, 022309 (2002).

[3] T. E. Keller and M. H. Rubin, Phys. Rev. A **56**, 1534 (1997); W. P. Grice and I. A. Walmsley, *ibid.* **56**, 1627 (1997).

[4] C. K. Hong, Z. Y. Ou, and L. Mandel, Phys. Rev. Lett. **59**, 2044 (1987).

[5] W. P. Grice, R. Erdmann, I. A. Walmsley, and D. Branning, Phys. Rev. A **57**, R2289 (1998); Y.-H. Kim, V. Berardi, M. V. Chekhova, and Y. Shih, *ibid.* **64**, 011801(R) (2001); M. Atatüre, A. V. Sergienko, B. M. Jost, B. E. A. Saleh, and M. C. Teich, Phys. Rev. Lett. **83**, 1323 (1999).

[6] E. Knill, R. Laflamme, and G. J. Milburn, Nature (London) **409**, 46 (2001).

[7] Y.-H. Kim, S. P. Kulik, M. V. Chekhova, W. P. Grice, and Y. Shih, Phys. Rev. A **67**, 010301(R) (2003).

[8] M. Fiorentino, G. Messin, C. E. Kuklewicz, F. N. C. Wong, and J. H. Shapiro, Phys. Rev. A **69**, 041801(R) (2004).

[9] W. P. Grice, A. B. URen, and I. A. Walmsley, Phys. Rev. A **64**, 063815 (2001).

[10] Z. D. Walton, M. C. Booth, A. V. Sergienko, B. E. A. Saleh, and M. C. Teich, Phys. Rev. A **67**, 053810 (2003).

[11] V. Giovannetti, L. Maccone, J. H. Shapiro, and F. N. C. Wong, Phys. Rev. Lett. **88**, 183602 (2002).

[12] V. Giovannetti, L. Maccone, J. H. Shapiro, and F. N. C. Wong, Phys. Rev. A **66**, 043813 (2002).

[13] F. König and F. N. C. Wong, Appl. Phys. Lett. **84**, 1644 (2004).

[14] E. J. Mason, M. A. Albota, F. König, and F. N. C. Wong, Opt. Lett. **27**, 2115 (2002).

[15] M. A. Albota and E. Dauler, J. Mod. Opt. **51**, 1417 (2004).

[16] C. K. Law, I. A. Walmsley, and J. H. Eberly, Phys. Rev. Lett. **84**, 5304 (2000).

[17] H. Fearn and R. Loudon, J. Opt. Soc. Am. B **6**, 917 (1989).

[18] C. Santori, D. Fattal, J. Vučković, G. S. Solomon, and Y. Yamamoto, Nature (London) **419**, 594 (2002).